International Journal of Automotive Technology, Vol. 7, No. 5, pp. 519–526 (2006)

Copyright © 2006 KSAE
1229-9138/2006/029-01

EFFECT OF FUEL STRATIFICATION ON INITIAL FLAME DEVELOPMENT: PART 1-WITHOUT SWIRL

I. Y. OHM* and C. J. PARK

Department of Mechanical Engineering and Graduate School of Energy & Environment, Seoul National University of Technology, Seoul 139-743, Korea

(Received 20 October 2005; Revised 9 May 2006)

ABSTRACT–For investigating the effect of fuel stratification on flame propagation, initial flame development and propagation were visualized under different axially stratified states in a port injection SI engine. Stratification was controlled by the combination of the port swirl ratio and injection timing. Experiments were performed in an optical single cylinder engine modified from a production engine and images were captured through the quartz window mounted in the piston by an intensified CCD camera. Firstly in this paper, the characteristics under no port-generated swirl condition, i.e. normal conventional case was studied. Under various stratified conditions, flame images were captured at the pre-set crank angles. These were averaged and processed to characterize the flames propagation. The flame stability was estimated by the weighted average of flame area and luminosity. The stability was also evaluated through the standard deviation of flame area and propagation distance, and mean absolute deviation of propagating direction. Results show that stratification state according to injection timing do not affect on the direction of flame propagation. The flame development and the initial flame stability are strongly dependent on the stratified conditions and the initial flame stability is closely related to the engine stability and lean misfire limit.

KEY WORDS : Initial flame, Stratification, Engine stability, Lean misfire limit, Visualization

1. INTRODUCTION

It is well known that the combination of fuel injection timing and port swirl determines the axial stratification state (Ohm and Cho, 2001). Hence, the stability and/or lean misfire limit of an engine is strongly affected by stratification in the port injection SI engine. Most of researches on stratification, however, have been carried in the limited area, such as measurement of local air-fuel ratio (AFR) at the specific points of combustion chamber, the investigation of lean misfire limit (LML) rather than the examination of the detailed process of stratification and the characteristics of flame propagation under stratified conditions (Quader, 1982; Matsushita, 1985a, 1985b; Takeda, 1985; Ando and Akishino, 1991; Horie, 1992; Ohm *et al.*, 1994; Ohm *et al.*, 1998).

In the internal combustion engines, especially in the reciprocating one having moving piston, it is very difficult to predict or simulate the whole stratification process due to highly turbulent flow and complex flow-to-flow interactions. Although the detailed mechanism and final state of stratification are known through fuel concentration measurement(Ohm *et al.*, 1994; Ohm and Cho, 2001), there is little data to investigate the effect of stratification on the real flame development and propagation, which is closely related to engine performance.

In this study, the characteristics of flame development and propagation have been investigated by means of visualization under various stratified conditions to examine the effect of flame propagation on engine performance. Firstly, in this paper the characteristics under no port-generated swirl condition, i.e., normal conventional case are studied.

2. EXPERIMENTAL METHOD AND APPARATUS

2.1. Optical Engine

The experiments were performed in an optical single cylinder engine modified from a production engine and images were captured by an intensified CCD camera through the quartz window mounted in the piston. Detailed port shapes and the engine specifications can be found in references (Ohm *et al.*, 1998).

Figure 1 shows the schematics of experiment and Table 1 represents the engine specifications. The visualization was performed for all ports. Compressed natural gas (CNG) and gasoline were used as fuel to investigate the

*Corresponding author. e-mail: iyohm@snut.ac.kr

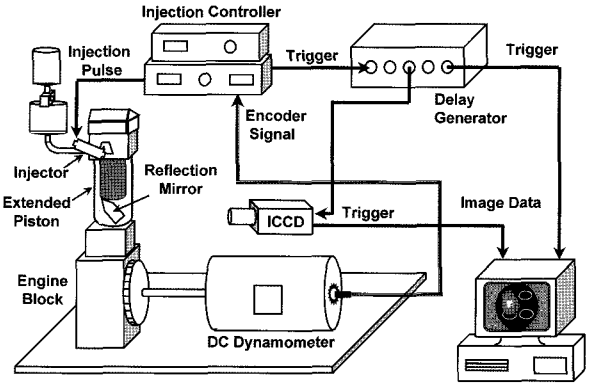

Figure 1. Schematics of visualization system.

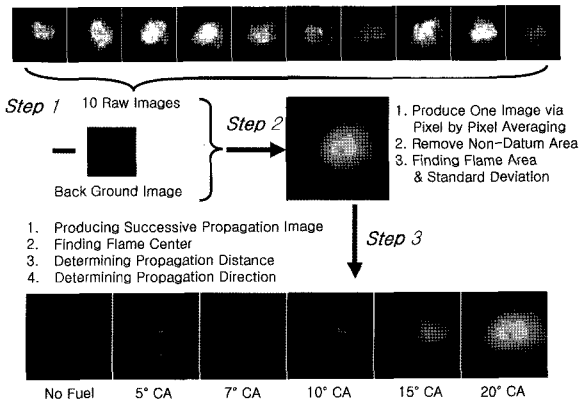

Figure 2. Raw image processing procedure.

Table 1. Engine specifications.

No. cylinder	1
No. of intake valve	2
No. of exhaust valve	2
Valve timing (IVO/IVC, EVO/EVC)	5/35 35/5
Combustion chamber	Semi-Wedge
Bore	73.5 mm
Stroke	83.5 mm
Max. Valve lift	7.2 mm

effect of fuel phase.

2.2. Experimental Condition

Experiments were operated at 1500 rpm under fully warm-up conditions. Ignition timing was fixed at BTDC 35° CA (Crank Angle) which is the same as that of engine performance tests. The engine load condition was 1.5 bar BMEP (Break Mean Effective Pressure) and the injection timing was varied from intake ATDC 10° CA to 360° CA for inducing different stratified conditions as the basis of reports that reverse axial stratification does take place when the injection is performed during the intake stroke under no swirl condition, in which air-fuel ratio (AFR) of upper cylinder region is leaner than total or average AFR (Ohm *et al.*, 1994; 1998). The reference of the timing is the end of injection pulse. The flame images were captured by an ICCD camera (Intensified CCD, Stanford Computer Optics 4 Quick 05A). The optical engine was run at slightly lean AFR condition (λ=1.14 for gasoline and λ=1.17 for CNG

The images were captured at 5°, 7°, 10°, 15° and 20° CA (crank angle) after the ignition. At each capturing timing, 10 images were acquired to produce an average image. To compare the images, the gain and exposure time of ICCD camera were fixed and no additives were mixed to fuel. As there was no light source except the flame, captured images contained little noise. The images were averaged and processed to characterize the flame. The flame stability was estimated by the weighted average of flame area and luminosity.

2.3. Image Processing

Figure 2 shows procedure of raw image processing. For analyzing image data quantitatively, the pixel data of captured image firstly were converted to number values. Since the images captured through ICCD have gray 8-bit scale, numbers varying from 0 to 255 corresponding to the intensity have been allocated for each pixel.

As mentioned above, because no additive was mixed in fuel and blind curtain was used to cut off outer light source, there was little noise except flame light. To eliminate background noise more completely, however, the pixel data of background image, which was capture under no firing condition, was subtracted from that of raw images. (step 1) After reading all images, which were under same injection timing and crank angle, the images were averaged pixel by pixel. Zero value was allocated for the pixels having intensity values lower than pre-set threshold. After this, averaged numerical data was reconstructed to average images. During averaging images, the non-datum pixels such as reflected light being in outer range of transparent window were removed by assigning zero value (black) to those pixels.

For representing the quantitative flame propagation characteristics more precisely, it might be desirable to consider the flame area and intensity concurrently because of existence of weak-broad flames. Therefore the weighted flame area, in which the intensity of pixel is considered, and standard deviation of this area were calculated. The weighted flame area was defined as follows (step 2):

$$A=\frac{\sum_{1}^{N}\sum_{i=0}^{n} g_k}{N}$$

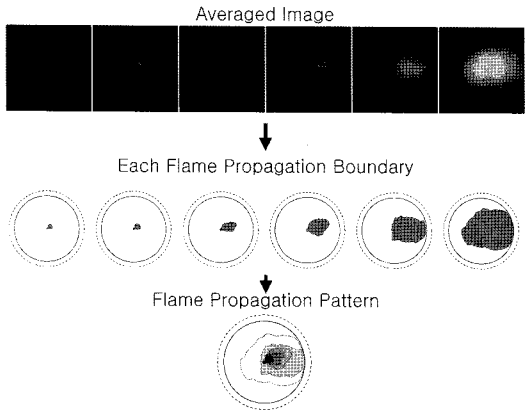

Figure 3. Finding propagation pattern procedure.

Where N : number of image
n : number of flame pixel
g_k : gray level of flame pixel

After this, all averaged images under the same injection timing were integrated to one images in which the images were successively arranged as a sequence of crank angle.

Since the simply averaged images have limitation in discussing characteristics of flame propagation quantitatively, the center of flame and distance of the center from the ignition point and its standard deviations were estimated. For the propagation direction is another important parameter in discussing the characteristics, the mean direction is estimated by simply averaging the data. On the other hand the deviation of propagation direction cannot be estimated by standard deviation because the direction has angle value that is periodical. It means the absolute value of this mean is meaningless. Therefore the mean average deviation (MAD) was calculated to deal with the propagation direction. (step 3)

In addition, the boundary of flame propagation was also determined for observing the propagation patterns more clearly. This boundary was determined only by the existence of flame and the intensity was not considered. The threshold of flame existing is that more than 5 raw images have flame pixel at that position.

This processing procedure is shown in Figure 3. In this figure, dotted circle line means real cylinder bore and solid one is the visualizing window boundary.

3. RESULT AND DISCUSSION

3.1. LML of Engine

Figure 4 shows the lean misfire limit (LML) of the engine as a function of the injection timing under no swirl condition in previous research (Ohm and Park, 2002). Because the injected fuel during the intake stroke exists mostly in the bottom of the cylinder under no swirl

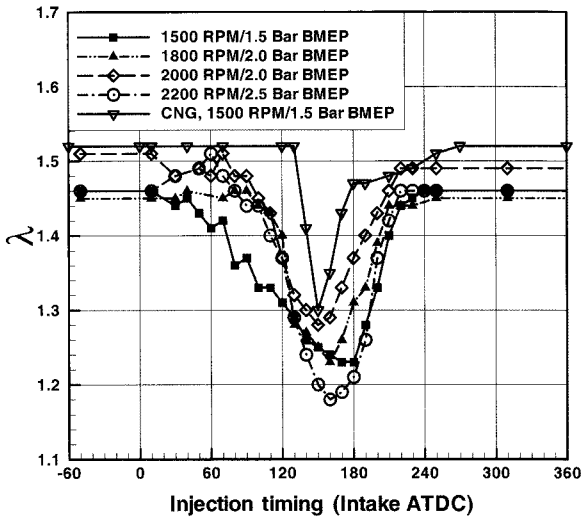

Figure 4. LML as a function of injection timing.

condition, the intake stroke injection lowers LML, i.e., the stability of engine. As shown in Figure 4, tendency of LML variation for gasoline and gaseous fuel (CNG) is similar. The main differences are as follows; firstly LML envelopes for CNG fuel is shifted to the retarded direction about 30° CA, secondly the range of injection timing for lower LML of CNG is narrower than that of gasoline. The difference in injection timing between gasoline and CNG disappears when considering CNG fuel arriving time at the valve is faster than that of gasoline as about 40° CA at 1500 rpm.

3.2. Raw Flame Image

Figure 5 shows the averaged flame images of gasoline fuel and Figure 6 shows those of CNG at each injection timing. In the figures, the angles on the right side are the injection timings and the bottom ones are crank angle after ignition. As shown in the figure, the developments of initial flames coincide with LML very well from the injection timing point of view: at the timing when LML is low (from ATDC 140–180° CA in gasoline and 120–160° CA in CNG), the visible flames are hardly observed. On the other hand, relatively clear flames are observed in other injection timings. It is also observed that there is no essential difference in gasoline and CNG flame propagation.

The details of propagating characteristics will be discussed with the quantitative data afterwards.

3.3. Flame Propagation Pattern and Direction

Figure 7 and 8 represent the propagation boundary of gasoline and CNG flame respectively. The white thick lines in the each pattern mean moving passage of flame centers; in determining which value the position and

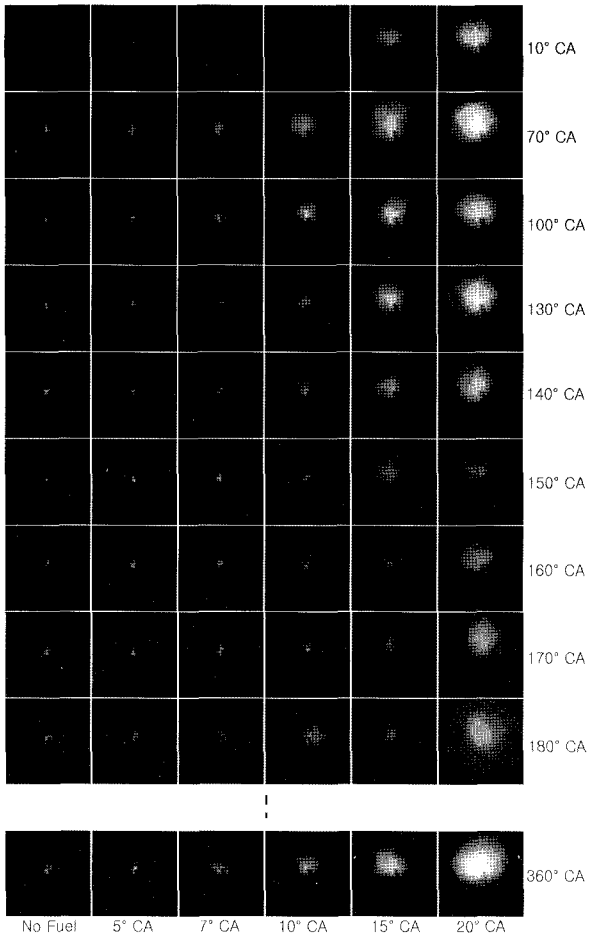

Figure 5. Flame propagation image according to injection timing when gasoline fueled.

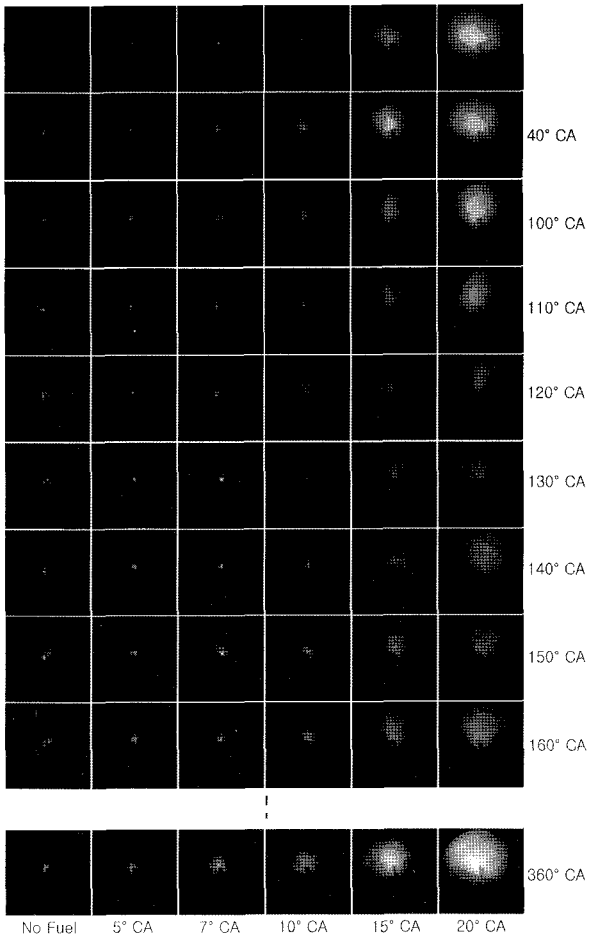

Figure 6. Flame propagation image according to injection timing when CNG fueled.

intensity are used concurrently. Comparing these figures with simple average images, it can be seen that the flames, which can be seen hardly in raw images, are more clearly visible as a result of finding the boundary. As mentioned above, the intensity of flame is not considered in defining the boundary, so the larger area could not mean strong flame absolutely. Nevertheless, it is observed that the stronger flame has larger propagation boundary on the whole.

In the figure, for the upper part of image is exhaust side and the lower is intake, the main propagation direction is exhaust side. Therefore, it is observed that each image shows similar trend of flame propagation in terms of direction and flame area regardless of injection timing and fuel.

To observe the propagation characteristics more closely, the flame center direction was calculated under the various bases. This result is shown in Figure 9. In the plot, firstly overall average (longest line) is estimated from all raw image, number of which is 750 respectively. Another averages, on the base of crank angle after ignition and the fuel injection timing (shortest line), are also derived. The crank angles in the figure mean the injection timings.

From the information of direction, several interesting phenomena could be observed.

As shown in figure, the overall directions of gasoline and CNG are slightly different as the direction of gasoline is 99° and that of the other is 103°. Because the number of data used in obtaining these averages is sufficiently large as 750, it might be considered that the 4° difference between two averages has some meaning. It is supposed that the different states of fuel distribution might cause this deviation.

In addition, some interesting phenomena might be found in this figure. Firstly, the direction of initial flame of gasoline starts right side of overall direction, then it moves counterclockwise toward left side of the direction as it grows. On the other hand, CNG flame moves from left to right in the clockwise direction. Secondly, the deviation of propagation according to crank angle after

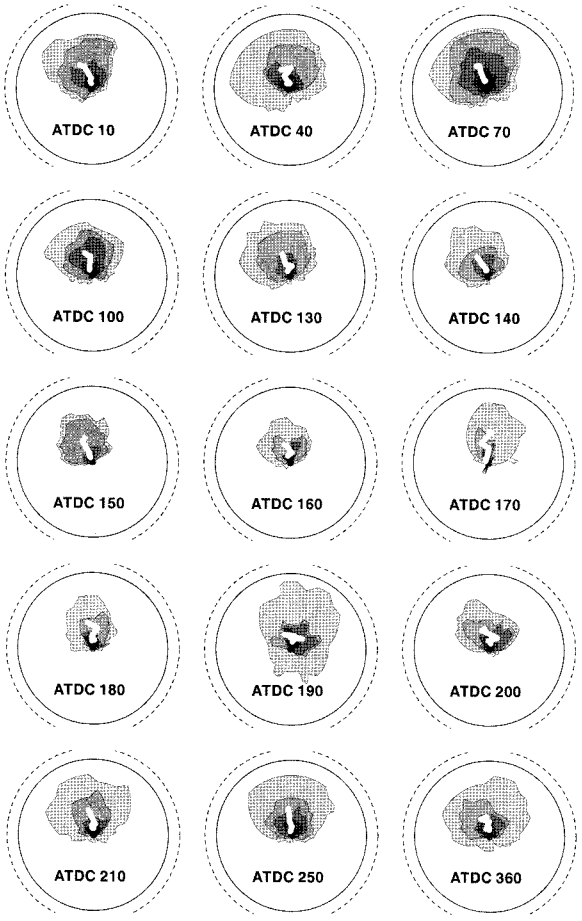

Figure 7. Flame propagation boundary according to injection timing when gasoline fueled.

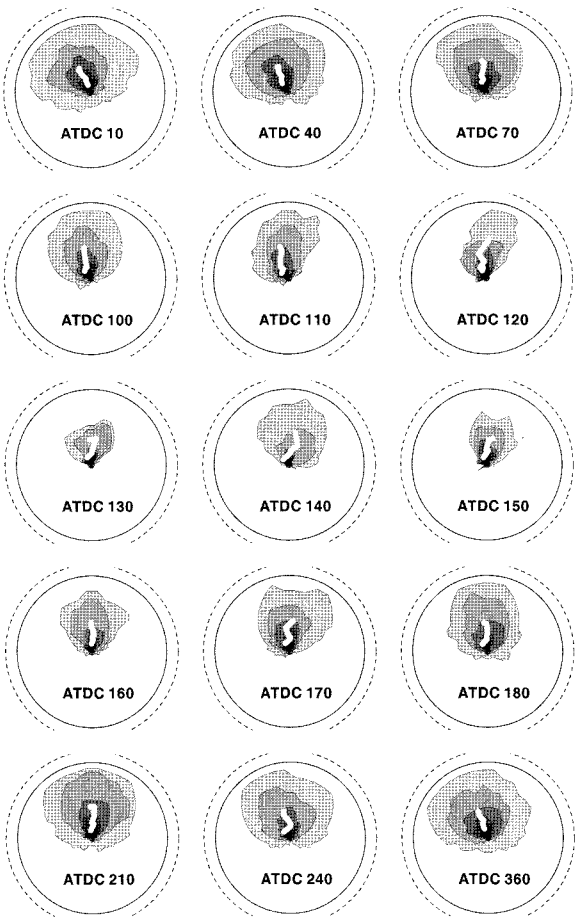

Figure 8. Flame propagation boundary (CNG).

ignition and injection timing is contrary to each fueling. The deviation of gasoline as a function of crank angle after ignition is lager than that of CNG, on the contrary the deviation of gasoline according to injection timing is smaller than that of CNG, i.e. the effect of injection timing on the propagation direction is more sensitive in CNG fueling.

Lastly, the deviations of propagation increase in the low LML range. The directions of change, however, are different from each fueling: the gasoline flames move to the left from the overall direction, on the other hand CNG flames go to the right in the low LML injection timing.

From the investigation of the flame propagation for all injection timing, it is revealed that the effects of stratified state and fuel phase on the pattern and direction are limited and minor. It is considered that the governing parameter of the pattern and direction might be in-cylinder flow because the main flow is tumble toward exhaust side at the end of compression stroke (i.e. initial firing stage), which coincides with the propagation direction very well. It is also observed that the stratification affects on the flame growing rate and size as shown in Figure 5–Figure 8.

3.4. Variations of Area and Direction

Figure 10 represents the weighted flame area, COV of this area, COV of propagation distance and MAD of the propagation direction of gasoline. From the figure, it is observed that the variation of weighted area according to the injection timing coincides with the pattern of LML very well; i.e., the higher LML, the larger area. It is also observed that COV of area tends to increase as the flame grows in low LML region. These observations are more apparent in CNG fuel (Figure 11). This might show the importance of initial flame for the stability and LML (Heywood, 1988; Stone, 1992). On the other hand, COV of distance reduces as the flame propagates except in lowest LML range. The reason of this reduction is supposed as follows. Because the main governing factor of propagating direction is in-cylinder flow, which goes from intake side to exhaust in this engine, the flame

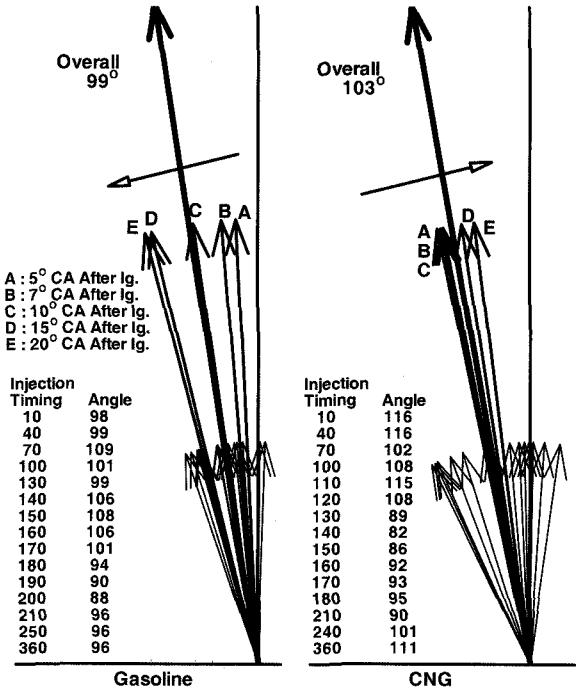

Figure 9. Direction of flame propagation.

moves from the spark plug to the cylinder wall. The radial boundary of flame, however, is limited by the cylinder wall instantly at the initial stage and the flame center could not move to outer due to this restriction so that the center of flame is practically fixed and the boundary expands along only lateral direction.

The MADs of direction show different trend in gasoline and CNG fueling. In case of gasoline, there is no certain tendency except that it has relatively large value in low LML range. That of CNG, however, decreases on the whole as the flame grows. Especially, the value is very large immediately after the ignition, but it reduces considerably in low LML range as the flame propagates. It is considered that better mixture preparation of gaseous fuel (CNG) causes a reduced flame-to-flame variation during propagation process.

Comparing the pattern of flame area and deviations for gasoline with CNG, that of CNG is relatively simple and plain. It is also supposed that the difference of mixture preparation result in this variation.

4. CONCLUSIONS

From the visualization of initial flame development in an

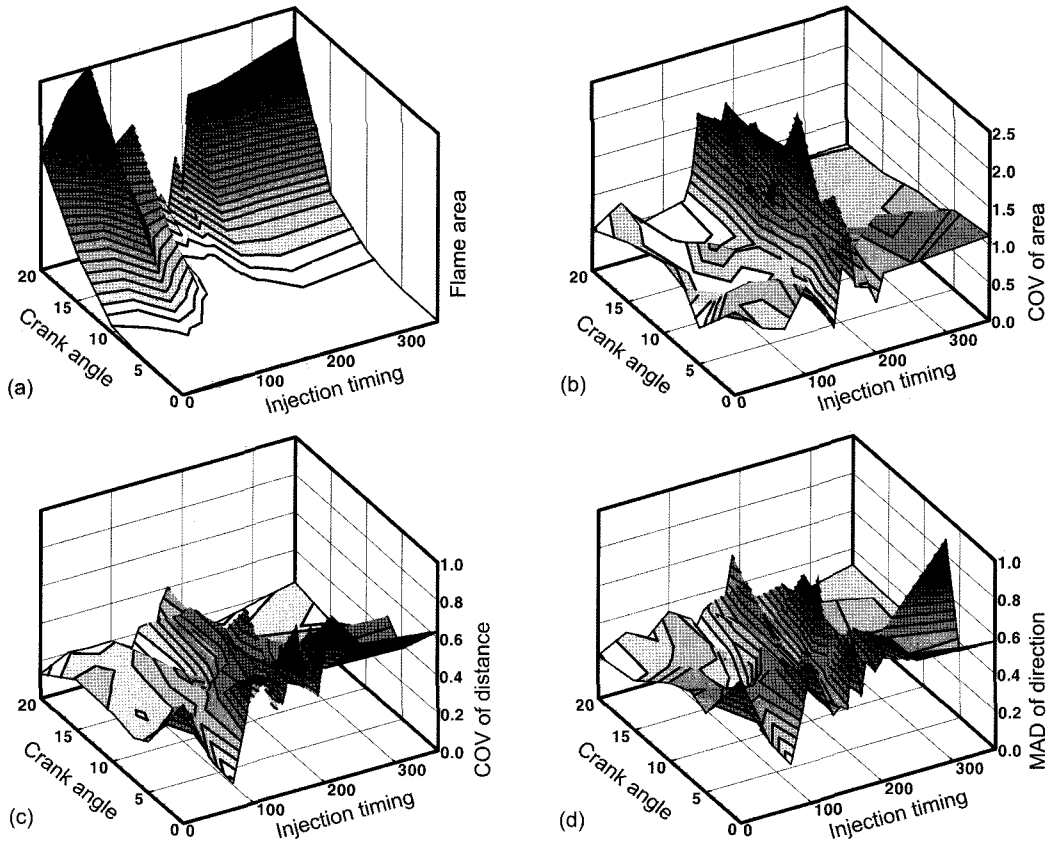

Figure 10. Flame area and deviation of gasoline fueling as a function of injection timing: (a) weighted flame area; (b) COV of weighted flame area; (c) COV of flame propagation distance; (d) MAD of propagation direction.

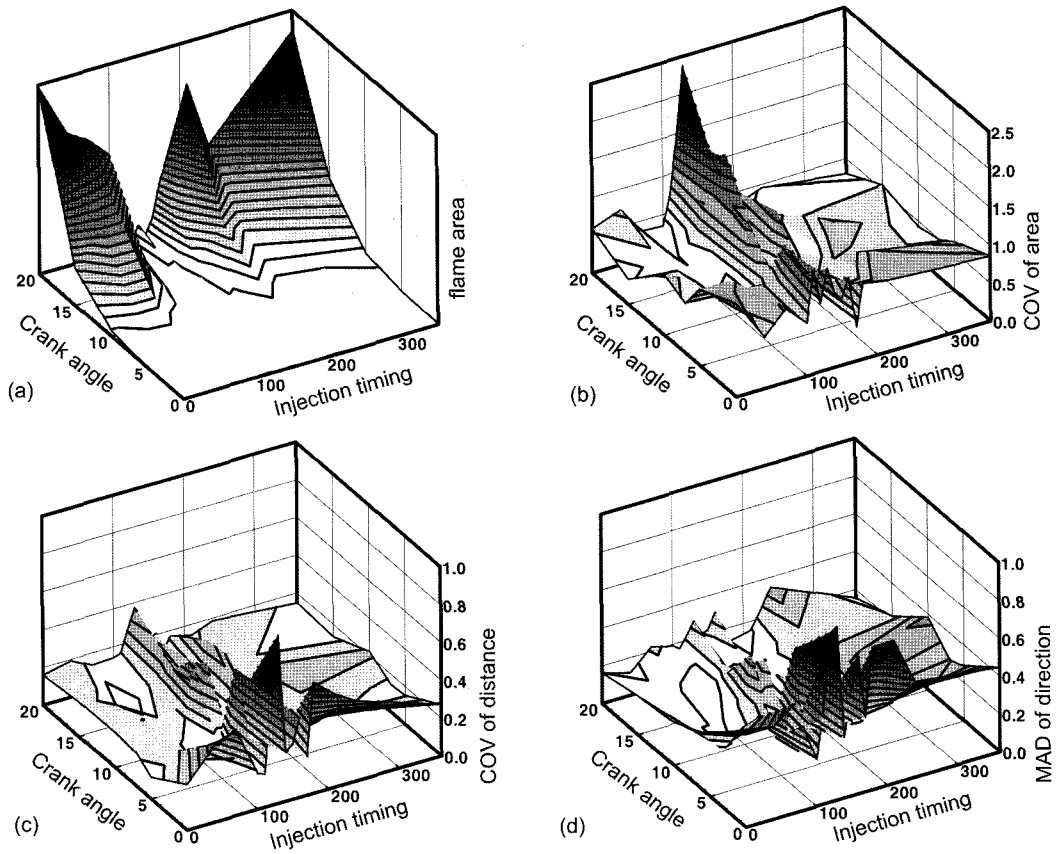

Figure 11. Flame area and deviation of CNG fueling as a function of injection timing: (a) weighted flame area; (b) COV of weighted flame area; (c) COV of flame propagation distance; (d) MAD of propagation direction.

optical single cylinder engine, the followings have been observed;

(1) Area of the initial flame and COV of that coincides with lean misfire limit very well from the injection timing point of view.
(2) Phase of fuel do not affect on the initial flame development patterns, the propagating direction and the flame area.
(3) Initial flame propagating direction is affected by the in-cylinder flow.
(4) Stratified condition, which is governed by the fuel injection timing, decides flame growing rate.
(5) Over whole propagating direction is slightly different form each fueling.
(6) Change of for gasoline fueling during flame growth is larger than that for CNG.
(7) Change of propagating direction due to injection timing for gasoline fueling is smaller than that for CNG.
(8) Changes of propagating direction according to flame growth and injection timing show opposite trend between gasoline and CNG fueling.
(9) COV of propagating distance reduces as the flame grows except in lowest LML range.
(10) MAD of direction for gasoline has no certain tendency, however that for CNG decreases as the flame propagates in low LML range.

REFERENCES

Ando, H., Akishino, K. (1991). Concept of lean combustion by barrel-stratification. *SAE Paper No.* 912207.

Heywood, J. B. (1988). *Internal Combustion Engine Fundamentals*. MacGraw-Hill. New York. 371–375.

Horie, K. (1992). The Development of high fuel economy and high performance four-valve lean burn engine. *SAE Paper No.* 920455.

Matsushita, S. (1985a). Development of the Toyota lean combustion system. *SAE Paper No.* 850044.

Matsusita, S. (1985b). Effects of helical port with swirl control valve on the combustion and performance of SI engine. *SAE Paper No.* 850046.

Ohm, I. Y., Ahn, H. S., Lee, W. J., Kim, W. T., Park, S. S. and Lee, D. U. (1994). Development of HMC axially stratified lean combustion engine. *1993 SAE Trans.* **103, 3,** 1298–1311.

Ohm, I. Y., Jeong, K. S. and Jeung, I. S. (1998). Effects of

injection timing on the lean misfire limit in an SI engine. *1997 SAE Trans.* **106, 3,** 42–55.

Ohm, I. Y. and Cho, Y. S. (2001). In-cylinder fuel behavior according to fuel injection timing and port characteristics in an SI engine: Part I-Without swirl. *Trans. Korean Society of Automotive Engineers* **9, 2,** 19–27.

Ohm, I. Y. and Park, C. J. (2002). Experimental study on axial stratification process and its effects (1), *J. Mechanical Science and Technology* **16, 11,** 1457–1469.

Quader, A. A. (1982). The axially-stratified-charge engine. *SAE Paper No.* 820131.

Stone, R. (1992). *Introduction to Internal Combustion Engines 2nd Edn.*. MACMILLAN. London. 72–74.

Takeda, K. (1985). Toyota central injection (CI) system for lean combustion and high transient response. *SAE Paper No.* 851675.